ISSN 0020-1685, Inorganic Materials, 2010, Vol. 46, No. 12, pp. 1290–1295. © Pleiades Publishing, Ltd., 2010.
Original Russian Text © D.I. Bletskan, V.N. Kabatsii, M. Kranjčec, 2010, published in Neorganicheskie Materialy, 2010, Vol. 46, No. 12, pp. 1423–1429.

Photoelectric Properties of Ordered-Vacancy Ga_2Se_3 Single Crystals

D. I. Bletskan[a], V. N. Kabatsii[b], and M. Kranjčec[c]

[a] *Uzhgorod National University, Pidhirna ul. 46, Uzhgorod, 88000 Ukraine*

[b] *Mukachevo Institute of Technology, Uzhgorodska ul. 26, Mukachevo, 89600 Ukraine*

[c] *Department of Geotechnical Engineering, University of Zagreb, Hallerova Aleja 7, 42000 Varaždin, Croatia*

e-mail: crystal_lab457@yahoo.com

Received September 30, 2009

Abstract—We have studied the photoconductivity spectrum, thermally stimulated current, current–light characteristics, and temperature-dependent photocurrent in Bridgman-grown ordered-vacancy Ga_2Se_3 crystals. The observed temperature quenching of photoconductivity and two regions of its thermal activation in Ga_2Se_3 crystals are interpreted in terms of a multicenter recombination model which incorporates an *s*-channel of active recombination, *r*-centers of photosensitivity, and traps for nonequilibrium majority carriers.

DOI: 10.1134/S0020168510120034

INTRODUCTION

Gallium sesquiselenide, Ga_2Se_3, belongs to the $A_2^{III}B_3^{VI}$ family of compound semiconductors. An inherent feature of these materials is position disordering [1], a situation where the number of sites for a particular type of atom in the crystal lattice exceeds the number of atoms, and the distribution of the atoms over such sites is, at least partially, random. Moreover, the $A_2^{III}B_3^{VI}$ compound semiconductors exhibit a special type of polymorphism, related to the loose structure of their cation sublattices.

Ga_2Se_3, a typical representative of this family, exists in three polymorphs, α, β, and γ, which differ in the arrangement of the atoms and vacancies and in the degree of order [2–4]. The chalcogen atoms in the three polymorphs are in a slightly distorted close-packed arrangement, with the metal atoms in tetrahedral interstices. In the structure of the low-temperature phase α-Ga_2Se_3, the metal atoms are distributed over the tetrahedral sites at random. α-Ga_2Se_3 has a cubic (sphalerite) structure (sp. gr. $T_d^2 = F\bar{4}3m$, a = 5.422 Å [2]), in which one-third of the gallium sites are vacant. Because of the specific features of its structure, Ga_2Se_3 may undergo a disorder–order transition related to Ga vacancy ordering in the tetrahedra lattice. Indeed, prolonged (tens of days) annealing at temperatures below 970 K initiates a very slow transformation of the α-phase (cubic structure) to the β-phase (monoclinic structure), which involves vacancy ordering [3, 4]. The high-temperature cubic phase, γ-Ga_2Se_3, has the zinc blende structure, with no vacancy ordering, and differs in α parameter (5.463 Å) from the α-phase (sp. gr. $T_d^2 = F\bar{4}3m$) [2, 3].

The high concentration (~8×10^{27} m^{-3}) of stoichiometric vacancies in Ga_2Se_3 is primarily due to the facts that the valence condition is fulfilled and that the sphalerite structure has equal numbers of cation and anion sites. Cation vacancies are responsible for a number of unusual properties of the $A_2^{III}B_3^{VI}$, semiconductors, such as the anomalously high radiation hardness [5], slow relaxation processes and residual photoconductivity [6], and the lack of impurity conductivity in doped materials [7].

In recent years, gallium chalcogenides have been successfully used for chemical and electrical passivation of the surface of III–V semiconductors and IR/visible optoelectronic devices based on such materials [8].

All this is generating increasing research interest in the physical properties of the $A_2^{III}B_3^{VI}$, compounds, including Ga_2Se_3. The electronic structure of Ga_2Se_3 was calculated by Peressi and Baldereschi [9]. There are data on its edge-absorption [10, 11], photoconductivity [12, 13], IR absorption, and Raman spectra [14].

The purpose of this work was to systematically study the dc conductivity, thermally stimulated conductivity, and steady-state photoconductivity (PC) of Bridgman-grown Ga_2Se_3 crystals.

EXPERIMENTAL

Polycrystalline gallium sesquiselenide was prepared by direct elemental synthesis, by reacting stoichiometric amounts of Ga and Se with vibration stirring in silica

ampules sealed off under a vacuum of 10^{-3} Pa. Ga_2Se_3 single crystals were grown by directional solidification in a vertical Bridgman geometry in evacuated silica ampules and were annealed in the same furnace. Since growth and heat treatment conditions have a significant effect on the structural state (ordered or disordered) of the Ga_2Se_3 crystals, it was important to identify their structure.

This is commonly done by X-ray diffraction. At the same time, if all the possible structures (symmetries) and vibrational frequencies of crystals are known, the structure of a given crystal can be identified by Raman spectroscopy, a nondestructive, high-speed characterization technique.

Figure 1 shows an unpolarized Raman spectrum of a Ga_2Se_3 crystal. Comparison with Raman spectra of different polymorphs [14] provides conclusive evidence that our crystals have an ordered structure.

Samples for electrical and photoelectric measurements, in the form of plates $8 \times 5 \times 0.3$ mm in dimensions, were prepared by cleaving a bulk crystal, and coplanar contacts to their natural surface were made by indium solder. The dark current, photocurrent, and thermally stimulated current (TSC) were measured as a function of temperature in a nitrogen cryostat, the temperature in which could be varied linearly in the range 100–500 K. In TSC measurements, the heating rate was maintained constant at 0.3–0.7 K/s. Traps were filled by exposing the sample to band-gap light, which was selected from the spectrum of an incandescent lamp by appropriate optical filters. The current through the sample was measured by a standard electrometric amplifier whose output was fed to a computing system.

PC spectra were taken at an applied dc electric field no higher than 5 V/cm, using both modulated and unmodulated (constant) luminous fluxes. Steady-state PC was measured by an electrometric amplifier at an unmodulated luminous flux. In the case of modulated illumination, the signal from a load resistance was fed to the input of a selective amplifier (UNIPAN 232 B nanovoltmeter) connected to a synchronous detector and was stored in the computer for further processing. The desired wavelength was selected by a DMR-4 double monochromator.

RESULTS AND DISCUSSION

According to thermopower data, the Ga_2Se_3 single crystals were *n*-type. A number of samples cut from the same ingot were shown to range in 293-K dark resistivity from 5×10^7 to 1×10^8 Ω cm.

It might be expected that, because of the high density of native point defects (cation vacancies), the crystals would have low resistivity. However, the presence of stoichiometric vacancies in Ga_2Se_3 crystals has no effect on their electrical properties: as-grown crystals have high resistivity (in contrast to IV–VI layered compounds, in which the cation vacancies resulting from deviations from stoichiometry are electrically active, according to the homogeneity range, produce an impurity band, and make the crystals degenerate and low-resistivity [15]). Consequently, the structural cation vacancies in $A_2^{III}B_3^{VI}$ crystals differ radically from Ge and Sn vacancies in the IV–VI compounds, are not native point defects, and can be thought of as vacant interstitial sites.

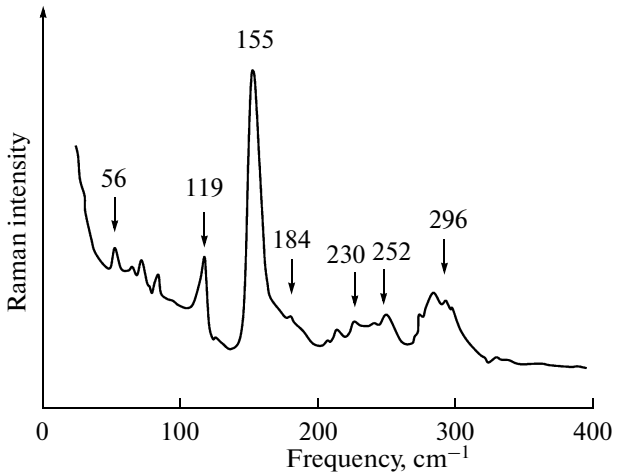

Fig. 1. 293-K Raman spectrum of a Ga_2Se_3 crystal.

According to the rule proposed by Suchet [16] for the formation of tetrahedral coordination in crystals, stoichiometric vacancies in the $A_2^{III}B_3^{VI}$ compounds should be considered zero-valence atoms. There are sp^3 bonds between the Ga and Se atoms, and four lone electron pairs are distributed between each vacancy and the four surrounding selenium atoms, so that the vacancy is formally linked to the anions as a normal cation [17, 18]. This configuration accounts for the semiconducting properties of the material, the electroneutrality of cation vacancies, and the low carrier mobility in comparison with other sphalerite-structure crystals [17, 18].

One possible reason for the high resistivity of Ga_2Se_3 crystals is the self-compensation of donors and acceptors during crystal growth. The process may involve both native defects and uncontrolled impurities. The formation of intrinsic (native) point defects is typically caused by deviations from stoichiometry resulting from the difference in vapor pressure between the components, as pointed out by Newman [3]. In reality, crystals can be contaminated with oxygen and silicon during synthesis and crystal growth in evacuated silica ampules as a result of the reaction between gallium and silica.

The Arrhenius plot of the dark current for one of our samples is presented in Fig. 2 (curve *1*). The temperature-dependent dark resistivity (obtained from the dark current, voltage drop across the sample, and its dimensions) shows exponential behavior, typical of compensated extrinsic semiconductors:

$$\rho = \rho_0 \exp(E_d/(kT)),$$

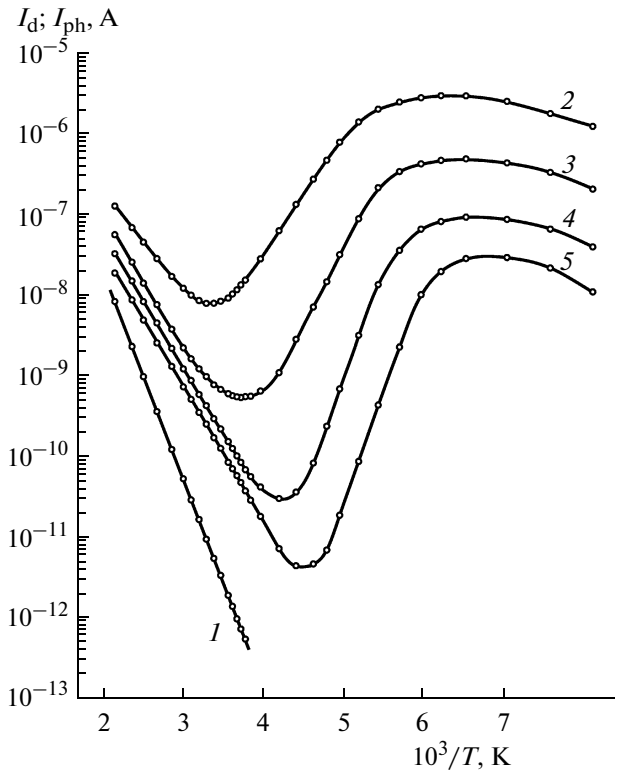

Fig. 2. Arrhenius plots of the (*1*) dark current I_d and (*2–5*) photocurrent I_{ph} at illuminances L = (*2*) 10^4, (*3*) 1.25×10^3, (*4*) 1.5×10^2, and (*5*) 40 lx.

where k is the Boltzmann constant, and E_d is the activation energy of donor centers in n-type crystals: $E_d = 0.52 \pm 0.02$ eV.

Typical unpolarized PC spectra of Ga_2Se_3 crystals at 293 and 100 K are presented in Fig. 3. The low-temperature PC spectrum (curve *1*) shows a strong band peaked at $h\nu_{max1} = 2.3$ eV, with a full width at half maximum (FWHM) of 0.3 eV, and a weak feature at $h\nu_{max2} = 1.97$ eV. To identify the origin of the PC peaks, we examined spectral dependences of the absorption coefficient (α) for the same sample around its fundamental absorption edge (Fig. 3, curves *4*, *5*). Comparison of the PC and edge absorption spectra (curves *1*, *4*) indicates that the higher energy peak ($h\nu_{max1} = 2.3$ eV) is located in the intrinsic region and is, therefore, due to band–band transitions. With increasing temperature, the intrinsic PC peak shifts to lower photon energies with a temperature coefficient $\partial E/\partial T = -1.6 \times 10^{-3}$ eV/K.

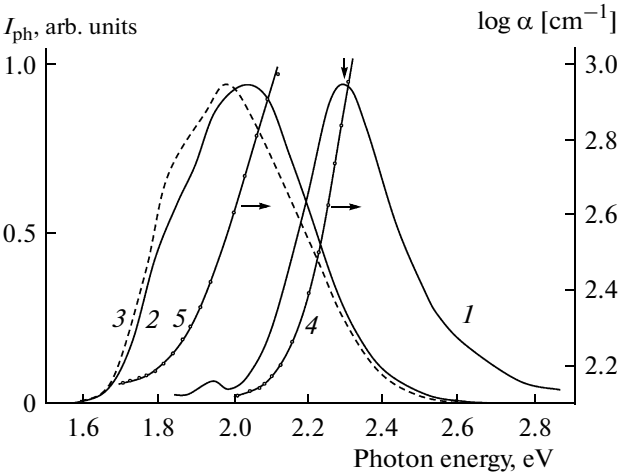

Fig. 3. (*1–3*) PC spectra taken with (*2*) modulated and (*1, 3*) unmodulated luminous fluxes and (*4, 5*) edge absorption spectra; (*1, 4*) 100 and (*2, 3, 5*) 293 K.

To gain more detailed information about the PC peaks near the intrinsic edge, we rely on the analysis of edge absorption spectra performed by Yoon et al. [10] and Mushinskii and Karaman [11]. Ga_2Se_3 single crystals are indirect-gap semiconductors with a 293-K band gap $E_{gi} = 1.95$ eV. In addition, there are direct allowed optical transitions at $k = 0$ with $E_{gd} = 2.07$ eV at 293 K. Therefore, the maximum at $h\nu = 1.97$ eV in the 293-K PC spectrum obtained under unmodulated illumination (Fig. 3, curve *3*) is due to indirect band–band transitions. The PC spectrum obtained under modulated illumination (curve *2*) shows a band centered at $h\nu_{max} = 2.05$ eV, which is due to direct band–band transitions.

With increasing temperature, the impurity PC peak at $h\nu_{max2} = 1.97$ eV, due to the optical ionization of r-centers, also shifts to lower photon energies, and its intensity increases. Because of the smaller temperature coefficient of the impurity band compared to the intrinsic band, they overlap at room temperature, and the impurity PC shows up as a shoulder at ~1.85 eV on the low-energy side of the intrinsic band under both modulated and unmodulated illumination (Fig. 3, curves *2, 3*). In this spectral region, Mushinskii and Karaman [12] identified an individual band centered at 1.8 eV (690 nm). Abdal-Rahman and Shaikh [13] reported a PC spectrum consisting of one, broad band, covering the range 1.7–2.5 eV; that is, the intrinsic and impurity bands were not separated.

The above differences in the behavior of the impurity PC band between Ga_2Se_3 crystals prepared in different laboratories can be understood in terms of the degree of cation order. Indeed, as pointed out by Palatnik et al. [19], vacancy ordering in Ga_2Se_3 is a rather slow process. For this reason, crystals grown by different techniques and heat-treated under different conditions may differ in diffraction pattern, even if they have the same structure.

In studies of steady-state PC decay kinetics under "light-shock" excitation such that the concentration of photogenerated nonequilibrium carriers exceeded the concentrations of traps and photosensitivity centers (slow recombination centers) [20], the photocurrent decay curve was shown to consist of two distinct portions, differing in decay time: $\tau_s = (5–8) \times 10^{-5}$ s and $\tau_r = (1–5) \times 10^{-3}$ s. Moreover, the Ga_2Se_3 crystals had $\chi \ll 1$. According to Lashkarev et al. [20], this is an indication that the photocurrent decay times τ_r and τ_s

are autonomous times of electron recombination through the *r*- and *s*-centers.

Thus, PC decay analysis indicates that the recombination of nonequilibrium carriers in Ga_2Se_3 crystals is governed by fast *s*-centers and slow ("sensitizing") *r*-centers. The presence of slow recombination *r*-centers in Ga_2Se_3 crystals is supported by temperature-dependent steady-state PC measurements.

The Arrhenius plots of the photocurrent under band-gap excitation at different illuminances (L varied by ~10^4 times) are presented in Fig. 2 (curves *2*–*5*). The $I_{ph}(10^3/T)$ curves are seen to have one region of temperature quenching of photocurrent (TQP) and two regions where the photocurrent increases with temperature (activation). At the highest illuminance, TQP begins at 190–200 K (curve *2*), the temperature range of TQP is $\Delta T =$ 80–90 K, and the photocurrent drops by two to three orders of magnitude. The TQP onset depends on illuminance, L, and shifts to higher temperatures with increasing L.

Studies of the temperature quenching of PC at different band-gap excitation intensities make it possible not only to verify criteria for when this effect can be observed experimentally but also to determine the depth of the *r*-center relative to the valence band (E_{vr}) and the ratio of the carrier capture cross sections for this center. According to Bube [21], the condition for the transition from high sensitivity to the region where the sensitivity decreases both with increasing temperature at a constant excitation intensity and at a constant temperature is given by

$$\ln n_{max} = \ln\left(N_c \frac{S_p}{S_n}\right) - \frac{E_{vr}}{kT_{max}}, \quad (1)$$

where n_{max} is the carrier (electron) concentration corresponding to breaks in $I_{ph}(T)$, N_c is the effective density of states in the conduction band, S_p and S_n are the carrier capture cross sections for the sensitizing *r*-center, E_{vr} is the depth of the sensitizing *r*-center relative to the valence band top, and T_{max} is the peak quenching temperature.

Figure 4 shows the Arrhenius plots of the photocurrent corresponding to the breaks. From the slope of these lines, the energy position of the *r*-center was determined to be $E_{vr} = 0.51$ eV.

Another, independent method for determining the depth of the *r*-center is to measure $\Delta L/L$ as a function of $1/T$ [20], where ΔL is the change in the excitation intensity, L, needed to maintain a constant electron concentration n upon changes in temperature in the range of temperature quenching of PC:

$$\frac{\Delta L}{L} = \frac{g_s B}{C_{rn} n} = g_s Q_v \frac{C_{rp}}{nC_{rn}} \exp\left(-\frac{E_{vr}^T}{kT}\right). \quad (2)$$

Here, g_s and g_r are the fractions of the total carrier recombination flux through the *s*- and *r*-centers, respectively ($g_r = 1 - g_s$); C_{rp} and C_{rn} are the probabilities of hole and electron capture at the *r*-center; and Q_v is the statistical factor for the valence band. From the slope of the Arrhenius plot of $\frac{\Delta L}{L}$, the depth of the *r*-center was determined to be $E_{vr} = 0.51$ eV.

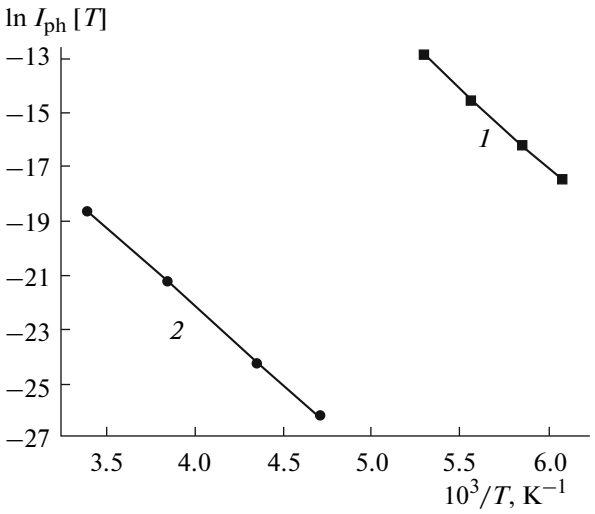

Fig. 4. Arrhenius plots of the photocurrent corresponding to transitions (*1*) from a higher to lower sensitivity and (*2*) from the reduced sensitivity to low sensitivity.

It can be seen in Fig. 2 that, at low temperatures (100–170 K), below the TQP region, there is a weak PC activation region. In the vast majority of wide-gap photoconductors, the low-temperature photocurrent activation is due to thermally induced charge transfer between traps for nonequilibrium majority carriers (*t*) and their recombination centers (*r*) [20].

To identify traps and determine their main parameters, we measured thermally stimulated currents in Ga_2Se_3 crystals.

Figure 5 shows TSC curves obtained at two different heating rates. In the temperature range 100–200 K, there is one peak, at $T = 148$ K, due to one trap. With increasing heating rate, the peak shifts to higher temperatures and becomes stronger.

To determine the depth of traps—their key parameter—from TSC curves, we used trap analysis techniques that are independent of the recombination mechanism (mono- or bimolecular) and carrier type in crystals (initial rise and Haering–Adams methods). We also used the FWHM of the TSC maximum [21, 22]. Independent of the type of trap (fast or slow), the initial portion of a TSC curve (below the peak onset temperature) can be described by

$$I_{TS} = \text{const} \exp(-E_t/(kT)).$$

From the slope of $\ln I_{TS}$ vs. T^{-1} and $\ln I_{TS}^{max}$ vs. T_m^{-1}, unrelated to the heating rate and frequency factor, the

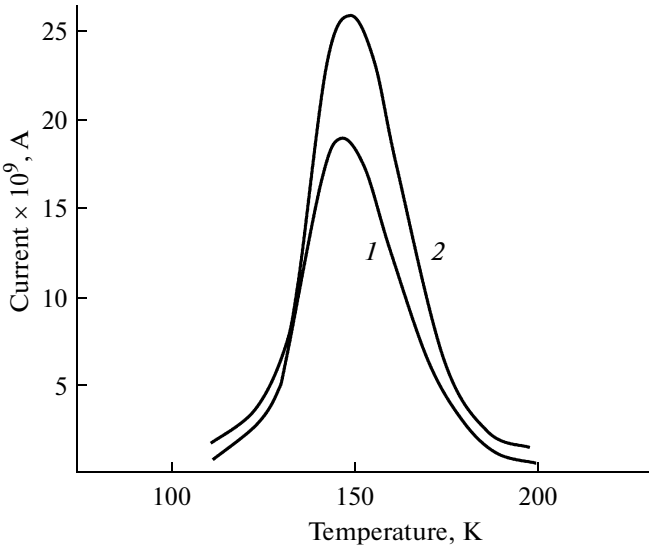

Fig. 5. TSC curves obtained at heating rates of (*1*) 0.3 and (*2*) 0.6 K/s.

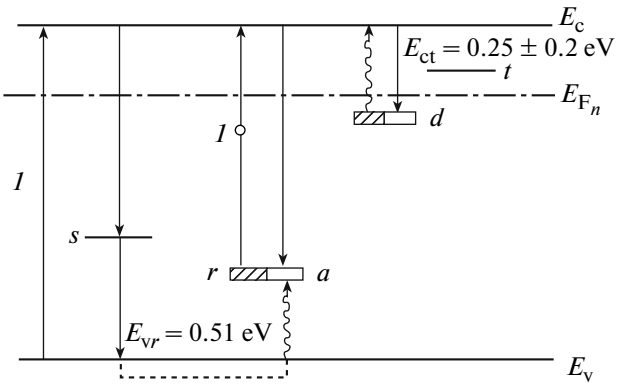

Fig. 6. Diagram of electron transitions in compensated ($R_d \geq R_a$) n-Ga_2Se_3 under band-gap and below-band-gap excitation. The solid arrows represent recombination transitions, and the wavy arrows represent thermal transitions; (*1*) optical generation.

trap depth was determined to be $E_{ct} = 0.25$–0.27 eV. From the FWHM of the maximum, the trap depth for second-order kinetics was 0.24 eV, in satisfactory agreement with the value derived from the initial rise. Thus, the level in question can be described by second-order kinetics, that is, carrier release is accompanied by significant retrapping. Using the formula for the trap concentration in this situation [22], we obtain 10^{16}–10^{17} cm^{-3}.

Thus, given that the temperature ranges of quenching and TSC decay differ very little (Figs. 2, 5), the observed increase in photocurrent with temperature below the TQP region is due to the emptying of the traps at $E_{ct} = 0.25 \pm 0.02$ eV.

The second region of photocurrent activation is observed above 230–300 K, that is, after the temperature quenching of the photocurrent reaches completion. The onset temperature for the photocurrent activation increases with excitation intensity. At low L, the photocurrent rises by four orders of magnitude. At high L, the temperature range of activation is narrower, and $I_{ph}(T)$ increases by just one order of magnitude. The high-temperature photocurrent activation may also be due to the thermal release of carriers from deeper traps. Because of the sharp rise in dark current above 230 K, we failed to detect a TSC peak attributable to carrier release from deeper traps, responsible for the photocurrent activation above 230 K. At the same time, Mushinskii and Pavlenko [23] observed not only a low-temperature TSC peak but also a peak at 273 K, that is, in the second region of photocurrent activation.

The current–light characteristics of Ga_2Se_3 crystals were found to be linear at low temperatures (below TQP onset) and superlinear in the region of strong quenching of the photocurrent. At still higher temperatures, there are two portions: linear and sublinear.

The observed effects and the parameters of recombination centers and traps inferred from steady-state PC and its decay kinetics enable electronic transitions in the system to be represented by an energy level diagram for three types of local centers (*r*- and *s*-centers of recombination and traps) in the band gap of Ga_2Se_3 (Fig. 6). According to this diagram, the band gap contains shallow donors (*d* and *t*) and deep recombination centers (acceptors *a*). The degree of their compensation is arbitrary, but the net donor concentration meets $\sum_i R_i \geq R_a$. The optical generation rate (acceptor *a* conduction band transition) is set by the absorption coefficient and incident photon flux density. The photogenerated nonequilibrium carriers (electrons in concentration Δn) may be captured by *a*-centers or by completely (*t*) or partially (*d*) compensated donors, acting as traps. The uncompensated donors ($N_{d0} = R_d - R_a$ at low temperatures) determine the temperature variation of the equilibrium electron concentration.

CONCLUSIONS

The single crystals grown in this study consist of β-Ga_2Se_3 as shown by Raman spectroscopy. Detailed studies of steady-state PC and its decay kinetics demonstrate that two processes typical of photosensitive semiconductors compete in Ga_2Se_3 crystals: temperature quenching and activation of PC. The current–light characteristics of the crystals are superlinear in the region of temperature quenching of PC. After exposure to a short band-gap light pulse, the photocurrent decay curve consists of two distinct portions.

The observed effects can be understood in terms of the proposed diagram of electron transitions involving three types of local centers (*r*- and *s*-centers of recombination and traps) in the band gap of Ga_2Se_3.

REFERENCES

1. Parsonage, N.G. and Staveley, L.A.K., *Disorder in Crystals,* Oxford: Clarendon, 1978.
2. Hanh, H. and Klingler, W., Über die Kristallstructuren von Ga_2S_3, Ga_2Se_3 und Ga_2Te_3, *Z. Anorg. Allg. Chem.*, 1949, vol. 259, nos. 1–4, pp. 135–142.
3. Newman, P.C., Ordering in $A_2^{III}B_3^{VI}$ Compounds, *J. Phys. Chem. Solids*, 1962, vol. 23, nos. 1–2, pp. 19–23.
4. Lübbers, D. and Leute, V., The Crystal Structure of β-Ga_2Se_3, *J. Solid State Chem.*, 1982, vol. 43, pp. 339–345.
5. Gal'chinetskii, L.P., Katrunov, K.A., Koshkin, V.M., and Kulik, V.N., Radiation Resistance of the IR Transmittance of Ga_2Se_3 Crystals, *At. Energ.*, 1981, vol. 50, no. 2, pp. 144–145.
6. Abdulaev, G.B., Tagiev, B.G., Niftiev, G.M., and Aliev, S.I., Slow Relaxation and Residual Photoconductivity in Ga_2Se_3 Single Crystals, *Fiz. Tekh. Poluprovodn.* (Leningrad), 1982, vol. 16, no. 9, pp. 1640–1642.
7. Koshkin, V.M., Gal'chinetskii, L.P., and Korin, A.I., Electrical Conductivity of Heavily Doped $B_2^{III}C_3^{VI}$ Semiconductors, *Fiz. Tekh. Poluprovodn.* (Leningrad), 1971, vol. 5, no. 10, pp. 1983–1985.
8. Sysoev, B.I., Bezryadin, N.N., Kotov, G.I., et al., Passivation of the GaAs (100) Surface with (110) $A_2^{III}B_3^{VI}$ Gallium Chalcogenides, *Fiz. Tekh. Poluprovodn.* (S.-Peterburg), 1995, vol. 29, no. 1, pp. 24–32.
9. Peressi, M. and Baldereschi, A., Structural and Electronic Properties of Ga_2Se_3, *J. Appl. Phys.,* 1998, vol. 83, no. 6, pp. 3092–3095.
10. Yoon, C.-S., Park, K.-H., Kim, D.-T., et al., Optical Properties of Ga_2Se and Ga_2Se_3:Co^{2+} Single Crystals, *J. Phys. Chem. Solids*, 2001, vol. 62, pp. 1131–1137.
11. Mushinskii, V.P. and Karaman, M.I., *Opticheskie svoistva khal'kogenidov galliya i indiya* (Optical Properties of Gallium and Indium Chalcogenides), Chisinau: Shtiintsa, 1973.
12. Mushinskii, V.P. and Karaman, M.I., *Fotoelektricheskie i lyuminestsentnye svoistva khal'kogenidov galliya i indiya* (Photoelectric and Luminescent Properties of Gallium and Indium Chalcogenides), Chisinau: Shtiintsa, 1975.
13. Abdal-Rahman, M. and Shaikh, H.A., Photoelectric Properties of Ga_2Se_3 Single Crystals, *J. Phys. D: Appl. Phys.,* 1996, vol. 29, pp. 889–892.
14. Finkman, E., Tauc, J., Kershaw, R., and Wold, A., Lattice Dynamics of Tetrahedrally Bonded Semiconductors Containing Ordered Vacant Sites, *Phys. Rev. B: Solid State*, 1975, vol. 11, pp. 3785–3794.
15. Bletskan, D.I., *Kristallicheskie i stekloobraznye khal'kogenidy Si, Ge, Sn i splavy na ikh osnove* (Crystalline and Glassy Si, Ge, and Sn Chalcogenides and Related Alloys), Uzhgorod: Zakarpat'e, 2004, vol. 1.
16. Suchet, J.P., *Chimie physique des semi-conducteurs,* Paris: Dunod, 1962.
17. Zhuze, V.P., Sergeeva, V.M., and Shelykh, A.I., Electrical Properties of In_2Te_3, a Structurally Imperfect Semiconductor, *Fiz. Tverd. Tela* (Leningrad), 1960, vol. 2, no. 11, pp. 2858–2871.
18. Abrikosov, N.Kh., Bankina, V.F., Poretskaya, L.V., et al., *Poluprovodnikovye khal'kogenidy i splavy na ikh osnove* (Semiconducting Chalcogenides and Their Alloys), Moscow: Nauka, 1975.
19. Palatnik, L.S., Belova, E.K., and Koz'ma, A.A., Concerning Anomalous Effects in X-Ray Diffraction Patterns of Gallium and Its Alloys, *Dokl. Akad. Nauk SSSR*, 1964, vol. 159, no. 1, pp. 68–71.
20. Lashkarev, V.E., Lyubchenko, A.V., and Sheinkman, M.K., *Neravnovesnye protsessy v fotoprovodnikakh* (Nonequilibrium Processes in Photoconductors), Kiev: Naukova Dumka, 1981.
21. Bube, R., *Photoelectronic Properties of Semiconductors*, Cambridge: Cambridge Univ. Press, 1992.
22. Vertoprakhov, V.M. and Sal'man, E.G., *Termostimulirovannye toki v neorganicheskikh veshchestvakh* (Thermally Stimulated Currents in Inorganic Materials), Novosibirsk: Nauka, 1979.
23. Mushinskii, V.P. and Pavlenko, N.M., Thermally Stimulated Conductivity of $Ga_{2x}In_{2(1-x)}Se_3$ Crystals, *Fiz. Tekh. Poluprovodn. (Leningrad),* 1971, vol. 5, no. 1, pp. 189–191.

МУКАЧІВСЬКИЙ ДЕРЖАВНИЙ УНІВЕРСИТЕТ

89600, м. Мукачево, вул. Ужгородська, 26
тел./факс +380-3131-21109
Веб-сайт університету: www.msu.edu.ua
E-mail: info@msu.edu.ua, pr@mail.msu.edu.ua
Веб-сайт Інституційного репозитарію Наукової бібліотеки МДУ: http://dspace.msu.edu.ua:8080
Веб-сайт Наукової бібліотеки МДУ: http://msu.edu.ua/library/